Angular Random Walk Estimation of a Time-Domain Switching Micromachined Gyroscope

Andrew B. Sabater
Paul Swanson

SSC Pacific
San Diego, CA 92152-5001

SSC Pacific
San Diego, California 92152-5001

K. J. Rothenhaus, CAPT, USN
Commanding Officer

C. A. Keeney
Executive Director

ADMINISTRATIVE INFORMATION

SB

EXECUTIVE SUMMARY

Microelectromechanical systems (MEMS) gyroscopes could potentially be used in low cost, size, weight, and power (CSWaP) navigation-grade inertial navigation units, but current solutions cannot be used due to issues with angular random walk (ARW), bias instability, and scale factor instability. While there are methods to address issues with bias and scale factor instability, with the commonly used demodulation schemes, ARW is limited by the ability to produce resonators with very high quality factors. Given that producing resonators with very high quality factors is challenging, the time-domain switching micromachined gyroscope (TDSMG) is proposed. As opposed to the conventional means that employ electrostatic sensing, the motion of the proof mass is detected through switches at known locations. In conjunction with an accurate time interval analyzer, the TDSMG is capable of estimating rotation rate in a low-noise fashion that is robust to environmental effects. Thus, it is expected that it will have low bias and scale factor instabilities. Simulated ARW performance of a particular incarnation of the TDSMG is studied. It is found that with narrow-bandwidth restrictions, near navigation-grade performance is capable without the need for the resonator to have a very high quality factor.

CONTENTS

Figures

Tables

1. INTRODUCTION

The primary metrics that prohibit the use of microelectromechanical systems (MEMS) gyroscopes for navigation-grade inertial navigation units (IMUs) are angle random walk (ARW), bias instability, and scale factor instability. The need for MEMS gyroscopes is due to their decreased cost, size, weight, and power (CSWaP) constraints compared to current navigation-grade solutions. Note that to avoid confusion, while in a statistical context a random walk describes a particular type of random process, ARW is used herein to quantify the effects of white, or Gaussian, noise processes on the rate estimate of a gyroscope. The accepted theory about how to mitigate effects associated with thermomechanical noise, and thus lower ARW, quality factors on the order of a million are needed [1], [2]. While resonators with quality factors on the order of a million have been demonstrated in laboratory settings [3], navigation-grade ARW has only been demonstrated in high-vacuum systems ($<10\,\mu$Torr) that would be challenging to implement in a portable system [4]. Other means of reducing ARW, such as increasing the amplitude of the drive mode, can be problematic. For electrostatically transduced devices, which is one of the more common methods used with MEMS, large oscillations can introduce nonlinear behavior such as electrostatic softening or pull-in [5]. Relatively recent works have demonstrated that virtual carouseling [2] and closed loop scale factor [6] can be used to significantly reduce bias and scale factor instability, respectively. However, it is important to note that it is unknown if these methods will degrade the performance of a gyroscope with navigation-grade ARW.

The proposed time-domain switching micromachined gyroscope (TDSMG) seeks to address ARW, bias instability, and scale factor instability by using measurements from discrete trigger events that occur when the proof mass of the gyroscope passes known locations. It builds upon work done with the time-domain switching accelerometer that can estimate acceleration without the need for adjustable parameters [7]. In addition, instead of the sensor's resolution being limited by noise from the amplifiers [5], it is controlled by the computational precision of the means used to estimate rotation rate and by the precision time is measured. There are no issues associated with noise from feedback electronics as feedback is not needed [4] and noise associated with the readout electronics is minimal as the TDSMG is sensed using digital means. By using highly accurate time interval analyzers and knowledge of the position of the triggers, determining angular rate as well other parameters (i.e., frequency mismatch, time constant mismatch, etc.) can be formulated as a parametric system identification problem.

Unlike classically designed MEMS gyroscopes, timing jitter contributes to the ARW of the TDSMG. Effects due to thermomechanical noise also play a role, but time-domain switching aids in mitigating this effect as large-amplitude oscillations, which would typically introduce nonlinear effects with electrostatically transduced devices, can be used. Thus, with the combination of large-amplitude oscillations, particular conditions for how the signal processing should be implemented, and the low jitter metrics of modern time interval analyzers (<1 ps), navigation-grade performance is capable. Moreover, since the signal processing used to determine angular rate is independent of parameters that are known to be sensitive to temperature or other environmental factors (e.g., variability of the natural frequency of the resonator with respect to temperature), it is expected that the bias and scale factor instability performance will be very good. The only parameter that is not directly estimated is the angular gain of the gyroscope. This parameter would need to be estimated with an initial calibration. Note that with structurally similar gyroscopes, such as the hemispherical resonator gyroscope, it was found that the angular gain was insensitive to temperature [8].

2. PARAMETRIC SYSTEM IDENTIFICATION BASED ON TIME-DOMAIN SWITCHING

Parametric system identification of linear systems has a vast body of literature [9]. Direct methods, or methods that allow the underlying physical parameters to be estimated, in general produce biased estimates. This bias tends to decrease as the sampling frequency increases as it allows the derivatives of the associated underlying model to be more accurately represented. However, with the presented switch configuration, a relatively few number of samples are generated per oscillation of the gyroscope. While the switch configuration could be altered to increase the effective sampling rate, in general the variance of parameters estimated via direct methods tend to increase as the sampling frequency increases. Grey-box modeling [10] approaches could be used, however numerical experiments with its most recent implementation CTSM-R [11] demonstrated that it is vastly more sensitive to initial parameter estimates than the presented method.

As noted in the introduction, while electrostatic transduction is capable of producing high-rate measurements for the state of the gyroscope, it can introduce nonlinear effects and limit the displacement of the gyroscope. With time-domain switching, sensing the state of the gyroscope is instead based on detecting when the proof mass of the gyroscope passes proximity switches that are placed below the gyroscope. These switches are capacitive, but other ones such as tunneling current switches could be used. While this does not provide a high-rate of state detection relative to the natural frequency the gyroscope, it allows the device to operate with larger displacements. Thus, instead of requiring extremely-high quality factors to achieve navigation-grade ARW, ARW can be lowered by operating with much larger displacements than conventional MEMS gyroscopes.

Presented in this section is a means to estimate not only the rotation rate of the gyroscope, but other parameters associated with imperfections of the gyroscope, based on a finite number of trigger events. Fundamental to this method is the validity of Lynch's model [12], which governs the modal, coordinates of class two Coriolis vibratory gyroscopes (CVGs) [13]. Class two CVGs are characterized by the having two or more degenerate modes, or modes that possess the same natural frequency, that are coupled via the Coriolis force. A crude schematic of the class two CVG considered in this study is shown in Figure 1. As will be discussed in greater detail in the following section, in the absence of any imperfections the mode shapes of the device can be represented by the ones shown in Figure 2. In practice, the modes of the gyroscope may not be aligned to the switches, and that in general, the damping axis will also not be aligned to the switches. However, Lynch's model accounts for this non-alignment. Thus, the modes shown in Figure 2 can still be used to represent the displacement of the ring. Note that positive displacements of the ring, or displacement away from the center of the ring, at 0° (switch 1) and 180° (switch 5) are associated with positive displacements of the first modal coordinate. Positive displacements of the ring at 90° (switch 3) and 270° (switch 7) are associated with negative displacements of the first modal coordinate. Similarly, positive displacements of the ring at 45° (switch 2) and 225° (switch 6) are associated with positive displacements of the second modal coordinate and positive displacements of the ring at 135° (switch 4) and 315° (switch 8) are associated with negative displacements of the second modal coordinate.
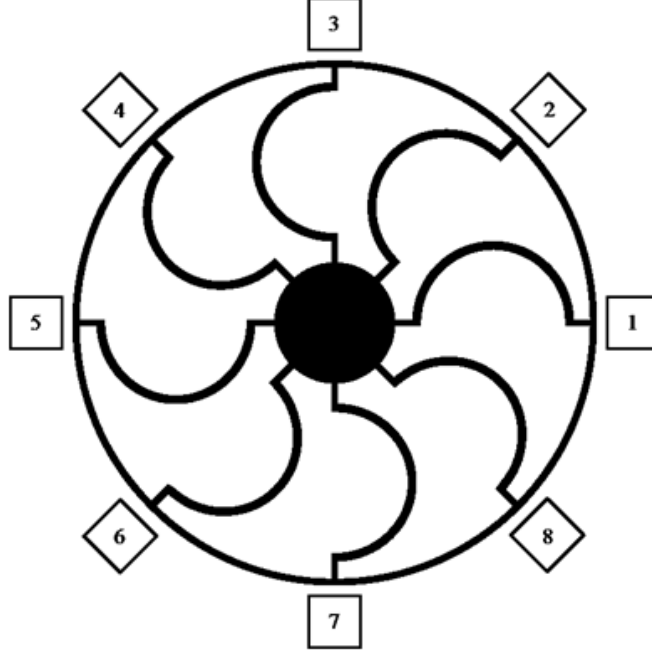
Figure 1. A crude schematic of the TDSMG. It consists of a ring that is supported by a central post with eight curved springs. The numbered boxes around the perimeter of the ring correspond to the switches used to sense the deflections of the ring.

Lynch's equations, refereed by Lynch as the equation of motion of the generic vibratory gyro, are reproduced below

$$
\begin{aligned}
&\ddot{q}_1 - k\left(2\Omega\dot{q}_2 + \dot{\Omega}q_2\right) + \frac{2}{\tau}\dot{q}_1 + \left(\omega^2 - k'\Omega^2\right)q_1 \\
&\quad + \Delta\left(\frac{1}{\tau}\right)\left(\dot{q}_1\cos(2\theta_\tau) + \dot{q}_2\sin(2\theta_\tau)\right) \\
&\quad - \omega\Delta\omega\left(q_1\cos(2\theta_\omega) + q_2\sin(2\theta_\omega)\right) = f_1, \\
&\ddot{q}_2 + k\left(2\Omega\dot{q}_1 + \dot{\Omega}q_1\right) + \frac{2}{\tau}\dot{q}_2 + \left(\omega^2 - k'\Omega^2\right)q_2 \\
&\quad - \Delta\left(\frac{1}{\tau}\right)\left(-\dot{q}_1\sin(2\theta_\tau) + \dot{q}_2\cos(2\theta_\tau)\right) \\
&\quad + \omega\Delta\omega\left(-q_1\sin(2\theta_\omega) + q_2\cos(2\theta_\omega)\right) = f_2
\end{aligned}
\tag{1}
$$

where q_1 and q_2 denote displacements of the first and second modal coordinates, respectively, and Ω is the angular velocity of the system. Since the gyroscope is designed such that the natural frequencies and time constants of the two modes are similar, these equations are written using average and difference values of the natural frequencies and time constants

$$\omega^2 = \frac{\omega_1^2 + \omega_2^2}{2},$$

$$\frac{1}{\tau} = \frac{1}{2}\left(\frac{1}{\tau_1} + \frac{1}{\tau_2}\right),$$

$$\omega\Delta\omega = \frac{\omega_1^2 - \omega_2^2}{2},$$

$$\Delta\left(\frac{1}{\tau}\right) = \frac{1}{\tau_1} - \frac{1}{\tau_2}. \tag{2}$$

For generality, f_1 and f_2 denote generalized forces for their respective modes, k denotes the angular gain that accounts for the Coriolis force and angular acceleration, and k accounts for centripetal forces. Finally, to handle misalignment of the mode shapes and a nontrivial principal damping axis, θ_ω and θ_τ have been introduced.
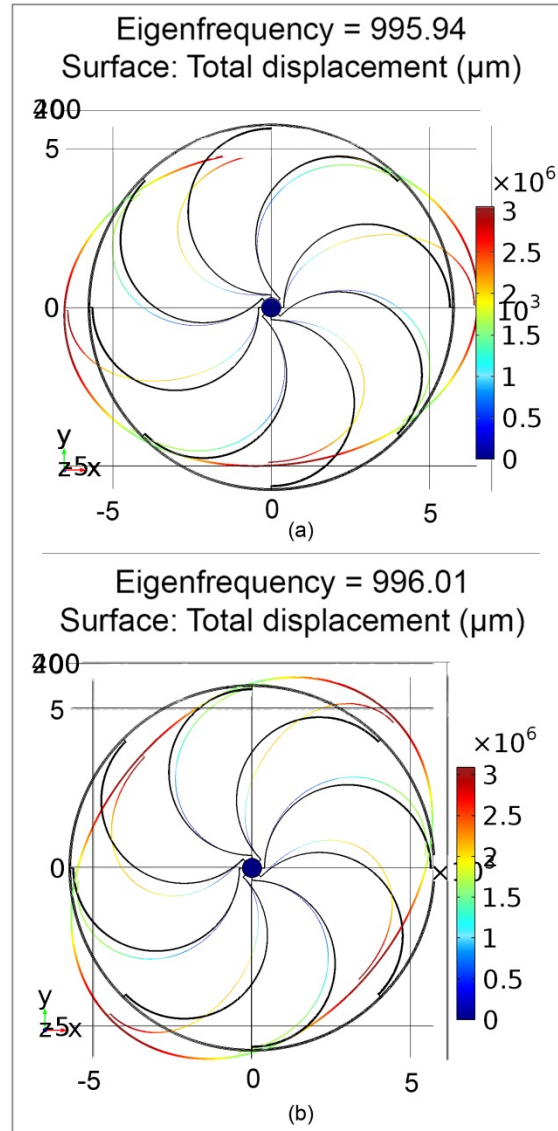
Figure 2. Mode shapes of the gyroscope corresponding to the first, degenerate flexural modes. These modes are used to sense rotation as they are coupled via the Coriolis force. Figure 2(a) and Figure 2(b) display positive displacements in the first and second modal coordinates, respectively. Note that these modes are not perfectly matched due to meshing issues with Comsol, but it is expected that with the actual device, a greater deviation of the natural frequencies will be observed due to fabrication imperfections and the anisotropic nature of silicon.

Ignoring effects associated with angular acceleration and centripetal acceleration and treating the quantity $2k\Omega$ as a single quantity, Lynch's model has seven parameters. Assuming that over a given period of time that these parameters are stationary and that only the free response of the gyroscope is considered, with four or more estimates for position, velocity, and acceleration, or state, of both modal coordinates at specific times, one could use linear least-squares methods to estimate these

5

parameters. That is, parameter estimates can be found by solving the following equation in a least-squares sense

$$
\begin{bmatrix} q_1 & -q_1 & -q_2 & \dot{q}_1 & \dot{q}_1 & \dot{q}_2 & -\dot{q}_2 \\ q_2 & q_2 & -q_1 & \dot{q}_2 & -\dot{q}_2 & \dot{q}_1 & \dot{q}_1 \\ & & & \vdots & & & \end{bmatrix}
\begin{bmatrix} \omega^2 \\ \omega\Delta\omega\cos(2\theta_\omega) \\ \omega\Delta\omega\sin(2\theta_\omega) \\ \dfrac{2}{\tau} \\ \Delta\left(\dfrac{1}{\tau}\right)\cos(2\theta_\tau) \\ \Delta\left(\dfrac{1}{\tau}\right)\sin(2\theta_\tau) \\ 2k\Omega \end{bmatrix}
=
\begin{bmatrix} -\ddot{q}_1 \\ -\ddot{q}_2 \\ \vdots \end{bmatrix}
\tag{3}
$$

where the ellipses are used to denote further measurements of the state. Note that since this is a linear least-squares problem, initial guesses for the parameters are not needed. If the state of the gyroscope was sensed at a sufficiently high enough rate, finite difference methods could be used to approximate the velocity and acceleration. In general, however, over a single period, one will only acquire four estimates for both modal coordinates. This is due to assuming that linear accelerations are insignificant such that redundant information is gleamed from switches on opposite sides of the ring (e.g., in the absence of linear accelerations, the proof mass will cross switches 1 and 5 at the same time). The presented means to estimate the state is to assume a solution for the free response of Lynch's equations and use the position of the triggers and the times at which the ring crosses the triggers to estimate parameters for the solution. That is, if Equation (1) can be rewritten in matrix form

$$
\dot{\mathbf{z}} = [A]\,\mathbf{z},
\tag{4}
$$

where $\mathbf{z} = [q_1 \; \dot{q}_1 \; q_2 \; \dot{q}_2]^T$, the homogeneous solution is of the form

$$
\mathbf{z} = \sum_{i=1}^{4} c_i \mathbf{v}_i e^{\lambda_i t},
\tag{5}
$$

where $\mathbf{v}_i$ and λ_i correspond to the i-th eigenvector and eigenvalue of $[A]$, respectively, and the c_i are used to account for initial conditions. As $[A]$ contains just real values and is of rank four, the eigenvectors and eigenvalues of $[A]$ come in complex conjugate pairs. Since only real initial conditions are of concern, it can be shown that the general form of the modal coordinates for the unforced version of Lynch's equations is

$$
\begin{aligned}
q &= A_1 e^{-\alpha_1 t}\cos\left(\frac{2\pi t}{T_1}\right) + B_1 e^{-\alpha_1 t}\sin\left(\frac{2\pi t}{T_1}\right) \\
&+ A_2 e^{-\alpha_2 t}\cos\left(\frac{2\pi t}{T_2}\right) + B_2 e^{-\alpha_2 t}\sin\left(\frac{2\pi t}{T_2}\right).
\end{aligned}
\tag{6}
$$

Thus, the proposed method of estimating all of the parameters in Lynch's equations consists of first acquiring a window of data sufficiently long enough to estimate the parameters for Equation (6). The velocity and acceleration of the modal coordinates can then be determined by differentiating Equation (6). With a minimum of four estimates for the state of both modal coordinates, one can solve Equation (3) for the parameters in Lynch's equations. Note that in the proposed method, it is

assumed that effects associated with linear acceleration are not considered. Given that the designed ring structure has a relative low natural frequency nominally at 1 kHz, sensitivity to linear acceleration might need to be addressed. However, assuming that linear accelerations result in slight translations of the center of the ring, one could account for linear accelerations by adding an offset term to Equation (6). Thus, while in the presented method, since linear accelerations are not considered, only the times the proof mass crosses switches 1 to 4 are needed. In practice, since linear accelerations may need to be considered, times from all eight switches would be needed.

To estimate the parameters in Equation (6), one needs at minimum eight trigger events from the switches that correspond to a given modal coordinate. Unlike Equation (3), the means used to determine these values is based on nonlinear least-squares methods. Thus, initial guesses for these parameters are needed. If close estimates for all of the parameters of Lynch's equations are known, the eigenvalues of $[A]$ and the corresponding estimates for α_1, α_2, T_1, and T_2 can be determined. With these estimates in hand, one can use linear least-squares to estimate A_1, B_1, A_2, and B_2. These values can then be used as initial ones for the fully nonlinear least-squares problem of determining α_1, α_2, T_1, and T_2 jointly with A_1, B_1, A_2, and B_2.

To determine close estimates for the parameters of Lynch's equations, one could use the results of previous iterations. For example, one could use the average of previous iterations to provide the needed close estimate. For the very first iteration, however, some initial calibration is needed. Based on the simulations conducted with the presented method, using averages of the previous 100 iterates as the close guess, the initial calibration values could be perturbed by 50% relative to the exact values with an insignificant effect on the resulting estimates. Thus, the proposed method is intensive to its initial calibration, but it does require some calibration.

In regards to implementation, with the estimates from Equation (6) in hand, one could use these fits to extrapolate. However, in the presented method, for a given window of data, the velocity and acceleration for q_1 are determined at the time that corresponds to the beginning of the window. For q_2, the velocity and acceleration are determined at the same time as q_1, but the window of data used to determine these values was selected such that the start of these two windows are as close as possible. Lastly, while provided the total number of estimates for both the position, velocity, and acceleration of q_1 and q_2 are greater than four and the window of data used to estimate the parameters in Equation (6) must be greater than eight, more state estimates and larger data windows help to mitigate effects with noise. In this study, it will be assumed that if the window of data used to estimate the parameters in Equation 6 contains N measurements, then N state estimates of q_1 and q_2 will be used to solve Equation (3). With this constraint, a total of $2N - 1$ trigger events from both modal coordinates are needed to complete a full iteration of the proposed method.

3. FINITE ELEMENT MODELING OF RESONATOR

This section details basic finite element modeling of the resonator used with the TDSMG. While it was done in part to validate that the first flexural mode is nominally at 1 kHz, more important was an estimate for the effects of thermomechanical noise. This was needed as the two primary sources of noise for the TDSMG are timing jitter from the time interval analyzer and thermomechanical fluctuations. However, for a given design of the resonator, while the effects of thermomechanical noise are constant, the relative effect of thermomechanical noise is dependent on the selection of the gap size of the triggers. This relative effect allows a comparison to the effects of timing jitter that will be discussed in the following section, and thus provide an overall study of the two primary sources of noise. The schematic of the resonator shown in Figure 1 exaggerates some of the features of the resonator that would be used in practice. The undeformed state of the resonator is shown in black in Figure 2. Device thickness is fixed at 500 μm and is assumed to be made of silicon. The radius of the ring is 5,700 μm and is 30 μm thick. The radius of the support post is 300 μm and the radius of the springs is 2,600 μm. The length of the posts connecting the springs to the support post is 100 μm. The width of the springs and connecting posts are 11 μm such that the springs are relatively soft.

As can be seen in Figure 2, natural frequencies of the first flexural modes were estimated in Comsol as approximately 996 Hz. These modes are not exactly matched due to issues with meshing, but given that in practice imperfections due to fabrication and the anisotropic nature of silicon, this mismatch is insignificant.

To estimate the effects of theromechanical noise, the modal stiffness of one of the employed modes is needed. From the equipartition theorem, one can estimate the mean square value of displacements due to theromechanical noise

$$\left\langle \frac{1}{2}Kq^2 \right\rangle = \frac{1}{2}k_BT,$$

(7)

where K is the modal stiffness, k_B is Boltzmann's constant, T is temperature in Kelvin, and $<\cdot>$ denotes the ensemble average. To estimate the modal stiffness, two opposing forces were applied near switches 1 and 5 and, in turn, the resulting displacement was estimated. This value was approximately 37.1 N/m. Assuming that temperature is 300 K, the standard deviation of displacements due to thermomechanical noise is $1.06 \times 10-5 \mu$m.

Since Lynch's equations are linear, it is possible to arbitrarily scale them. A convenient choice is selecting the displacement needed to cross the switches, or the switch gap, as 1. Thus, while the initial displacement of the ring needs to be greater than the switch gap, dividing the standard deviation of the displacement due to thermomechanical noise by the switch gap provides a normalized measure of thermomechanical noise. Assuming that the switch gap is 100 μm, as will be shown in the following section, this puts the effects of thermomechanical noise on par with 10 ps of timing jitter. A switch gap of 1000 μm would put the effects of thermomechanical noise close to having 1 ps of timing jitter, but it is likely that a displacement of 1000 μm would damage the ring. Thus the lower bound for the room temperature performance of the TDSMG discussed is near 10 ps of jitter response, but this bound could be pushed lower with lower temperatures or slightly larger switch gaps.

4. ANGULAR RANDOM WALK CHARACTERIZATION

This section details simulation of the TDSMG for the purposes of estimating the ARW. This is done by characterizing the behavior of the proposed system when the angular velocity is zero. The parameters used to simulate the device are given in Table I. The structure detailed in the previous section nominally has matched natural frequencies of 1 kHz; however, it is assumed that imperfections will exist with the real system. With the associated quality factors given in Table I, initial velocities of zero for both coordinates, and q_1 and q_2 are initially equal to $2g$ and $-2g$, respectively, where g is the switch gap, one can simulate for 8000 cycles before the oscillations of one of the modal coordinates is too small to be detected by the switches. This time corresponds to approximately 8 s. Note that if this system is implemented, a means to both set the initial conditions and detect when the oscillations can no longer be detected by the switches will need to be devised.

Table 1. Parameters used to simulate the TDSMG.

Parameter	Value
ω_1	$2\pi 1.02 \times 10^3 \frac{rad}{s}$
ω_2	$2\pi 0.98 \times 10^3 \frac{rad}{s}$
τ_1	$2\frac{50.3 \times 10^3}{\omega_1} \frac{1}{s}$
τ_2	$2\frac{49.7 \times 10^3}{\omega_2} \frac{1}{s}$
θ_ω	$5°$
θ_τ	$3°$
k	0.37

To generate simulated data from the switching events, standard numerical integration is not practical. The first dilemma with using numerical integration is that to generate an accurate solution, small time steps are needed. This, in turn, requires a long period of time to generate data. Note that most of this data is not needed as only switching events are used in the proposed method. The second dilemma is numerical integration does not directly provide a means to determine when the proof mass of the ring crosses the switches. Thus, as an alternative to numerical integration, an eigenvector/eigenvalue approach, is used. That is, the means used to generate simulated data employs the solution given in Equation (5). Since in simulation one knows all of the parameters in Lynch's model, it is simple to determine the eigenvectors and eigenvalues of $[A]$. With a given set of initial conditions, one can solve a system of linear equations for the c_i. The primary advantage of this method is that the state of the modal coordinates can be determined at arbitrary times. In conjunction with a root-finding algorithm, one can use the solution in Equation (5) to determine the times when the proof mass passes the switches.

Two different effects that influence ARW will be considered. The first is jitter associated the time interval analyzer. For simplicity, it is assumed that the error associated with the time interval analyzer is normally distributed with a zero mean and that this error corrupts measurements for when the proof mass passes the switches. Thus the value that is adjusted to account for error with the time interval analyzer is a standard deviation. It is worth noting that other sources of timing error may exist, such as effects associated with the selection of switching threshold and the velocity

of the modal coordinates, but these effects are not considered. The second is N, or the length of the data window used to estimate the parameters of Equation (6).

In an experimental context, ARW is typically estimated by fitting a model to an Allan variance measurement [14]. If the ARW is low, a rather long measurement is needed to acquire an accurate estimate of the Allan variance. For example, in [14] where a navigation-grade IMU was tested, data was acquired for two hours. However, since in effect the noise processes associated the TDSMG are Gaussian, the distribution of the estimated parameters is also Gaussian. Thus, the simulation only needs to be run long enough such that estimates for the associated standard deviations to converge. From [1], ARW is given by

$$\Omega_{rw} = \sqrt{\frac{\langle \theta_{\text{noise}}(t)^2 \rangle}{t}}, \tag{8}$$

where $\theta_{\text{noise}}(t)$ denotes the estimate of the rotation angle due to noise processes. Explicitly,

$$\theta_{\text{noise}}(t) = \int_0^t \Omega_{\text{noise}}(\tau) d\tau, \tag{9}$$

where Ω_{noise} refers to the estimate of the rotation rate due to noise processes. For large integration times, the ARW approaches a constant value

$$\frac{\langle \theta_{\text{noise}}(t)^2 \rangle}{t} \approx S_{\Omega_{\text{noise}}}(0), \tag{10}$$

where Ω_{noise} is the power spectral density of Ω_{noise}. In general, the integral of the power spectral density signal over the entire frequency domain is equal to its mean square value. If this signal has a zero mean, then this integral is equal to its variance. Moreover, if it assumed that this signal is sampled at a frequency f_s, the power spectral density is equal to zero for frequencies greater than $f_s/2$ and less than $-f_s/2$, and the power spectral density is equal to a constant, which is the case for Ω_{noise} since it is a Gaussian process

$$S_{\Omega_{\text{noise}}}(0) = \frac{\sigma_{\text{noise}}^2}{f_s}, \tag{11}$$

where $S_{\Omega_{\text{noise}}}$ is the standard deviation of the noisy rate estimate. Thus, accounting for the conversion from to (i.e., the scaling factor $10800/\pi$), ARW is estimated as

$$\Omega_{rw} = \frac{10800}{\pi} \frac{\sigma_{\text{noise}}}{\sqrt{f_s}}, \tag{12}$$

Due to the asynchronous nature rate estimates are generated, the value for f_s used is based on the average of the time differences from when the estimates arrive.

The proposed method does not lend itself well to providing a simple expression for σ_{noise}, and thus ARW, but Equation (12) does provide some design insights. The first is that while f_s is not equal to the natural frequency of the ring structures, it is approximately equal to four times this value. The natural frequency of the ring scales inversely with the square of the ring's radius (i.e., $f_n \propto 1/r^2$) [15], [16], thus if one can devise a means to mitigate the timing and signal processing issues associated with high frequencies, one path to decreasing ARW is decreasing the radius of the ring. The second is that with the assumed model for timing jitter, jitter is linearly related to the standard deviation of the position error of the modal coordinates. Position error in this context is defined as error associated with the position of the modal coordinates due to the time interval analyzer imprecisely recording when the proof mass crosses one of the switches. This can be seen in Figure 3 where increasing jitter by an order of magnitude increases the standard deviation of the position error by an order of magnitude. While not strictly applicable for the proposed method as position error disturbs the position, velocity, and acceleration of the modal coordinates differently, in general, for least-squares methods, the standard deviations of the estimated parameters scale linearly with the standard deviation of the noise. Thus it is expected that ARW scales linearly with jitter.
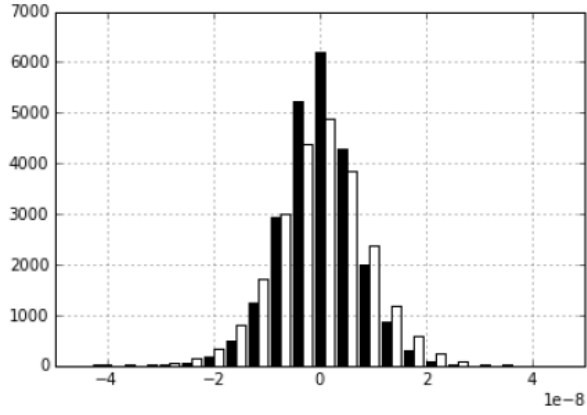
(a)
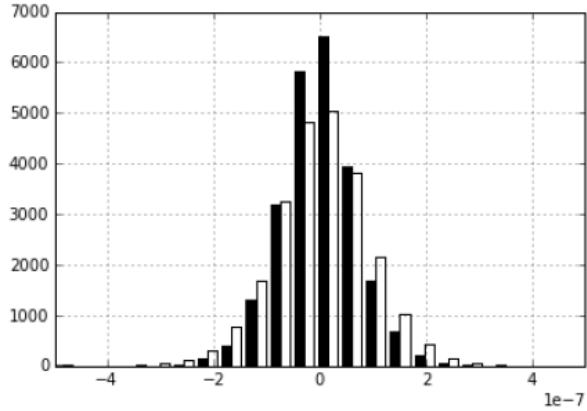
(b)

Figure 3. Histograms of the position error for the cases that jitter is 1 ps (Figure 3 (a)) and 10 ps (Figure 3 (b)). Position error is normalized such that $g = 1$. Note that black and white are used to denote the position error of q_1 and q_2, respectively.

Table 2 provides estimates for ARW for various values of jitter and data window length. These results are also shown graphically in Figure 4. As one might expect, increasing N or decreasing jitter decreases ARW. The predicted result that linearly increasing jitter linearly increases ARW is shown. In regards to N, these simulations suggest that there are diminishing returns on increasing N. The implication is then that arbitrarily increasing N may not be a practical means to getting to even lower values of ARW. However, for $N \geq 18$, Figure 4 shows a log-linear trend. Given the linear relationship with AWR and jitter, for $N \geq 18$, it is very simple to determine if a given jitter and N will meet a given ARW requirement. For $N < 18$, the breakdown of this trend is a reflection of challenges associated with fitting to Equation (6). Results for $N < 14$ are not shown as sporadic poor fits have yielded inconsistent estimates for AWR (i.e., angular rate estimates contain many outliers that skew the standard deviation estimate). Additional error handling could be introduced if operation with a low N is required, but it is not considered here.

Table 2. ARW estimates for various values of time interval analyzer jitter and N, the length of data used to fit to the model given in Equation (6).

	Jitter (ps)				
N	1	2	5	10	100
14	0.005072	0.010373	0.023565	0.047833	0.526467
16	0.010373	0.005577	0.014021	0.027456	0.276728
18	0.001867	0.003554	0.009266	0.017818	0.181893
20	0.001219	0.002527	0.006323	0.012475	0.125560
22	0.000934	0.001831	0.004547	0.009074	0.090761
24	0.000709	0.001407	0.003575	0.007045	0.069496

The $N \geq 18$ trend in Figure 4 also demonstrates a unique feature of the TDSMG: the ARW performance of the gyroscope is weakly coupled to the design of the mechanical structure, but strongly coupled to the performance of the time interval analyzer and how the data from the switches is processed. A limitation of the TDSMG is that increasing N not only introduces a delay in the sensor's response, but it also decreases its bandwidth. However, if the TDSMG is implemented where the data from the switches is processed via software or field-programmable gate array (FPGA), it might be possible to dynamically select N to balance ARW, delay, and bandwidth requirements. Thus, a single sensor could be tuned to suit a variety of applications. As noted in the previous section, for the designed resonator, the effects of thermomechanical noise for a switch gap of $100\,\mu$m corresponds to approximately 10 ps of timing jitter. For the 10 ps of timing jitter case with $N = 24$, ARW is approximately $0.007\ ^\circ/\sqrt{h}$, which is very close to the metrics that are considered navigation-grade. Thus, the TDSMG has the potential for navigation-grade performance, but without the need for a quality factor on the order of a million.
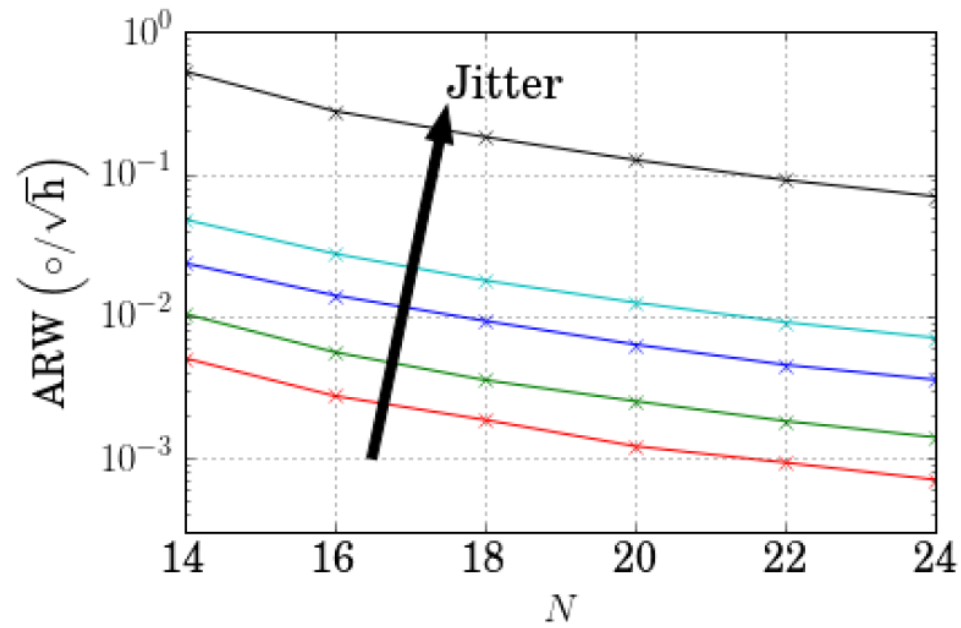
Figure 4. ARW as a function of N for various values of time interval analyzer jitter. Note that red (lowest), green, blue, cyan, and black (highest) are used to denote 1, 2, 5, 10, and 100 ps of jitter, respectively.

6. CONCLUSION

Estimates of the ARW of a TDSMG for various levels of noise were presented. The two dominant sources of noise are due to thermomechanical fluctuations and timing jitter associated with the needed time interval analyzer. Based on finite element simulations of the employed resonator, it is found that the effects of thermomechanical noise is on par with 10 ps of timing jitter. As such, the 10 ps of timing jitter ARW response of the TDSMG provides an approximate lower bound for the performance of the sensor. With this lower bound performance, in the case that the length of the needed number of measurements for a single mode of the resonator, or N, is equal to 24, ARW is very close to metrics that are considered navigation-grade. While the $N = 24$ case corresponds to a relatively narrow bandwidth, it would still be suitable for static rotation rate sensing applications, like gyrocompassing, or nearly-static rotation rate sensing, such as unmanned underwater vehicle navigation. Note, unlike other MEMS gyroscopes, once these narrow-bandwidth tasks are achieved (e.g., initializing the inertial navigation unit), it is possible to adjust the performance of the TDSMG to increase its bandwidth. While this would be done at the cost of increasing ARW, it would allow the TDSMG to be well suited for applications where the error due to initialization is of the greatest of concern (i.e., short duration). Future work on the TDSMG will focus on improving the needed signal processing to account for linear acceleration, developing a general model that will allow one to balance the effects of both thermomechanical noise and timing jitter for different resonator designs, and experimental validation of the sensor.

REFERENCES

1   R. Leland. 2005. "Mechanical-thermal Noise in MEMS Gyroscopes," *IEEE Sensors Journal*, vol. 5, no. 3, pp. 493–500.

2   A. Trusov, G. Atikyan, D. Rozelle, A. Meyer, S. Zotov, B. Simon, and A. Shkel. 2014. "Flat is not Dead: Current and Future Performance of Si-MEMS Quad Mass Gyro (QMG) System." *Proceedings of the Position, Location and Navigation Symposium (PLANS 2014, 2014 IEEE/ION)* (pp. 252–258). 5–8 May, Monterey, CA.

3   I. Prikhodko, S. Zotov, A. Trusov, and A. Shkel. 2011. "Sub-degree-per-hour Silicon MEMS Rate Sensor with 1 million Q-factor." *Proceeding of the 16th International Solid-State Sensors, Actuators and Microsystems Conference (Transducers'11)* (pp. 2809–2812). 5–9 June, Beijing, China.

4   D. Senkal, A. Efimovskaya, and A. Shkel. 2015. "Minimal Realization of Dynamically Balanced Lumped Mass WA Gyroscope: Dual Foucault Pendulum," *Proceedings of the 2nd IEEE International Symposium on Inertial Sensors and Systems (ISISS 2015)* (pp. 1–2). 23–26 March, Hapuna Beach, HI.

5   M. W. Putty. 1995. "Micromachined Vibrating Ring Gyroscope." Doctoral dissertation. University of Michigan, Ann Arbor, MI.

6   A. Trusov, I. Prikhodko, D. Rozelle, A. Meyer, and A. Shkel. 2013. "1 PPM Precision Self-Calibration of Scale Factor in MEMS Coriolis Vibratory Gyroscopes." *Proceedings of the 17th International Conference on Solid-State Sensors, Actuators and Microsystems (Transducers & Eurosensors 2013)* (pp. 2531–2534). 16–20 June, Barcelona, Spain.

7   P. Swanson, C. Tally, and R. Waters. 2011. "Proposed Digital, Auto Ranging, Self Calibrating Inertial Sensor." *Proceedings of the 10th IEEE Sensors Conference* (pp. 1457–1460). 28–31 October, Limerick, Ireland.

8   D. M. Rozelle. 2009. "The Hemispherical Resonator Gyro: From Wineglass to the Planets." *Proceedings of the 19th AAS/AIAA Space Flight Mechanics Meeting (AAS/AIAA 2009)* (pp. 1157–1178). 8–12 February, Savannah, GA.

9   H. Garnier, and L. Wang, Eds. 2008. *Identification of Continuous-time Models from Sampled Data*. Springer-Verlag, London, United Kingdom.

10 N. R. Kristensen, H. Madsen, and S. B. Jørgensen. 2004. "Parameter Estimation in Stochastic Grey-box Models," *Automatica*, vol. 40, no. 2, pp. 225–237.

11 R. Juhl. 2016. "CTSM-R - Continuous Time Stochastic Modelling for R."Available online at http://ctsm.info/. Accessed April 17, 2016.

12 D. Lynch. 1995. "Vibratory Gyro Analysis by the Method of Averaging." *2nd Saint Petersburg Conference on Gyroscopic Technology and Navigation* (pp. 26–34), 24–25 May, Saint Petersburg, Russia. Scientific Council of the Russian Academy of Sciences on the Traffic Control and Navigation Problems.

13 IEEE Aerospace and Electronic Systems Society. "IEEE Standard Specification Format Guide and Test Procedure for Coriolis Vibratory Gyros," IEEE Std 1431-2004, pp. 1–78.

14 N. El-Sheimy, H. Hou, and X. Niu. 2008. "Analysis and Modeling of Inertial Sensors Using Allan Variance," *IEEE Transactions on Instrumentation and Measurement*, vol. 57, no. 1, pp. 140–149.

15 S. S. Rao. 2007. *Vibration of Continuous Systems*. John Wiley & Sons, Inc. Hoboken, NJ.

16 F. Ayazi, and K. Najafi. 2001. "A HARPSS Polysilicon Vibrating Ring Gyro-scope," *Journal of Microelectromechanical Systems*, vol. 10, no. 2, pp. 169–179.

REPORT DOCUMENTATION PAGE

1. REPORT DATE *(DD-MM-YYYY)*	2. REPORT TYPE	3. DATES COVERED *(From - To)*
September 2016	Final	

4. TITLE AND SUBTITLE

Angular Random Walk Estimation of a Time-Domain Switching Micromachined Gyroscope

5a. CONTRACT NUMBER

5b. GRANT NUMBER

5c. PROGRAM ELEMENT NUMBER

6. AUTHORS

Andrew B. Sabater
Paul Swanson

5d. PROJECT NUMBER

5e. TASK NUMBER

5f. WORK UNIT NUMBER

7. PERFORMING ORGANIZATION NAME(S) AND ADDRESS(ES)
SSC Pacific
53560 Hull Street
San Diego, CA 92152–5001

8. PERFORMING ORGANIZATION REPORT NUMBER

TD 3308

9. SPONSORING/MONITORING AGENCY NAME(S) AND ADDRESS(ES)
SSC Pacific
Naval Innovative Science and Engineering Program
53560 Hull Street
San Diego, CA 92152–5001

10. SPONSOR/MONITOR'S ACRONYM(S)

11. SPONSOR/MONITOR'S REPORT NUMBER(S)

12. DISTRIBUTION/AVAILABILITY STATEMENT
Approved for public release.

13. SUPPLEMENTARY NOTES

This is a work of the United States Government and therefore is not copyrighted. This work may be copied and disseminated without restriction.

14. ABSTRACT

Microelectromechanical systems (MEMS) gyroscopes could potentially be used in low cost, size, weight, and power (CSWaP) navigation-grade inertial navigation units, but current solutions cannot be used due to issues with angular random walk (ARW), bias instability, and scale factor instability. While there are methods to address issues with bias and scale factor instability, with the commonly used demodulation schemes, ARW is limited by the ability to produce resonators with very high quality factors. Given that producing resonators with very high quality factors is challenging, the time-domain switching micromachined gyroscope (TDSMG) is proposed. As opposed to the conventional means that employ electrostatic sensing, the motion of the proof mass is detected through switches at known locations. In conjunction with an accurate time interval analyzer, the TDSMG is capable of estimating rotation rate in a low-noise fashion that is robust to environmental effects. Thus, it is expected that it will have low bias and scale factor instabilities. Simulated ARW performance of a particular incarnation of the TDSMG is studied. It is found that with narrow-bandwidth restrictions, near navigation-grade performance is capable without the need for the resonator to have a very high quality factor.

15. SUBJECT TERMS
microelectromechanical systems gyroscopes; navigation-grade inertial navigation; angular random walk characterization; time-domain switching micromachined gyroscope; parametric system identification; finite element modeling

16. SECURITY CLASSIFICATION OF:			17. LIMITATION OF ABSTRACT	18. NUMBER OF PAGES	19a. NAME OF RESPONSIBLE PERSON
a. REPORT	b. ABSTRACT	c. THIS PAGE			Paul Swanson
U	U	U	U	23	19B. TELEPHONE NUMBER *(Include area code)* (619) 553-7269

INITIAL DISTRIBUTION

SSC Pacific
San Diego, CA 92152-5001